*The Nucleus* ***59****, No. 1-4 (2022) 1-10*

*www.thenucleuspak.org.pk*

**The Nucleus**
**ISSN 0029-5698 (Print)**
**ISSN 2306-6539 (Online)**

# Impact of Inner Dopants on Structural, Optical and Mechanical Properties of Unadulterated L-Threonine Manganese Acetate

N. I. Ahamed [1*], D. B. Anburaj [2], G. Nedunchezhian [1]

[1]*PG and Research Department of Physics, Thiru. Vi. Ka. Govt. Arts College, Thiruvarur-3, Tamil Nadu, India*

[2]*PG and Research Department of Physics, D.G. Govt. Arts College (W), Mayiladuthurai-1, Tamil Nadu, India*

*(Affiliated to Bharathidasan University, Tiruchirappalli-24, Tamil Nadu, India)*

**ABSTRACT**

*Equal molar ratio of L-Threonine and manganese acetate (LTMA) and 0.2 Molar mass of $Zn^{2+}$, $Cd^{2+}$ and $Pb^{2+}$ doped LTMA single crystals were grown with their aqueous solution using the slow evaporation technique. These crystals were subjected to various studies such that single crystal X-Ray Diffraction Volume=530(4) $Å^3$ increased upto 540.8(4) $Å^3$, Powder X-Ray Diffraction, FTIR, UV-optical, Energy Dispersive and Microhardness studies. The cell length and interfacial angles $\alpha=\beta=\gamma=90^o$ of the grown crystals were determined. EDAX study confirms the placing of dopant ions $Zn^{2+}$, $Cd^{2+}$ and $Pb^{2+}$ in the host material LTMA. FTIR analysis reported the functional group and UV-Vis analysis carried out the optical behavior of the crystals. UV-Vis absorption spectrum analysis determines the increasing energy band gap from 4.6eV to 6.5eV and transmittance spectrum determines the lower cutoff wavelength of the grown crystals as 267nm for pure LTMA and around 200nm for doped LTMA. Mechanical behaviors of the grown crystals have been studied by Vicker's Microhardness Study and their roughnesses are reported.*

***Keywords:*** *Metallic Dopants, Single Crystal XRD, Powder XRD, EDAX, Microhardness MHD*

## 1. Introduction

In the present era, solution growth has prominent effect to make in technical and scientific advancement. A single crystal is a well known periodic arranging of atoms in a three dimensional space with equally repeated rules. Single crystals are the fundamental building blocks for modern technology. The well preparation of single crystal has good properties in advantages and applications. So, the regularity and uniformity of the single crystals transmit electromagnetic waves without losses. Crystal growth has controlled phase transformation and implies important natures, properties and qualities in materials science. Significant properties of crystal growth technology develop many excellent crystals, in ever growing applications in lasers, optical communication and data storage technology and so many application crystals. Hence, single crystals are very important and essentiality for further research and technology. In beginning days, the crystal growth is faces very difficulties in selecting methods and compound for related work. At that time materials have the very nonlinearity natures in characterizations as well as applications. After, it was enabled for the commercial development of single crystals with promising nonlinear optical properties. In short durations, large size crystals are essential for device fabrication with several fast growth methods. The present day demand is for large and high quality NLO, ferroelectric, piezoelectric single crystals and magnetic materials with minimum defects [1, 2]. To growing any application crystal, microscopic and macroscopic homogeneity is improvement is very important property. The synthesis of lot of crystals is the complicated process to attaining notable technical applications in the synthesis, growing process and analysis [3]. It has a connection between science and technology in making of regularly using device in the modern micro electronics industry. Most of the nonlinear optical crystals have proven as better single crystals to consist the applications such as non-linear optical nature, frequency compiling, piezo electric modulation, optical statistic movements, optical disobedient etc. Due to the recent advancements of these nonlinear optical materials has good quality organic crystals are grown as excitement in the last decade. The crystal growth is an art of growing crystal based on scientific principles to facilitate high technology applications in lasers, semiconducting devices, computers, magnetic and optical devices and pharmaceuticals, among others and needs expertise in chemistry, physics, optics and crystallography [4-9]. The growth of single crystals is both scientifically and technologically important. In this regards, amino acid based single crystals are very successful material to competing the above task [10]. Researcher lot of works completed using the amino acids such as L-Alanine, L-Proline, L-Arginine, L-Histidine and L-Valine etc.. [11-15].In recent, most of the exploration work has been done on the synthesizing and portrayal of semi natural crystal. Because of their wide optical applications, contrasted with different materials, amino corrosive blended natural crystal was intrigued to orchestrated. The search material has qualifies for the discovery of numerous natural NLO materials with high nonlinear natures and photonic applications. Authentically, it can utilize in uses of predominant quality precious stones. Like the semi natural precious stones, amino corrosive based semi natural gems were likewise has acceptable optical and non-direct optical natures. This

*Corresponding author: imthiiaz@yahoo.com

single crystal can likewise be developed from watery answer for the improved hardness and the warm steadiness. In this reference, unadulterated L-Threonine single gem and L-Threonine based Lithium Chloride (LTLC), Calcium Chloride (LTCC), Cadmium chloride (LTCC), Manganese chloride (LTMC) single precious crystal are developed and its characters likewise examined [14-18]. Afterward, L-Threonine Sulfate crystal like Lithium Sulfate (LTLS), Potassium Sulfate (LTKS), Zinc Sulfate (LTZS) and Copper Sulfate (LTCS) single precious crystal are developed and considered [19-22]. At that point, L-Threonine Cadmium Acetate (LTCA) and L-Threonine Zinc Acetate (LTZA) single precious crystal are developed [23-24]. In proceeds, this work finished with development on unadulterated L-Threonine Manganese Acetate (LTMA) and the Zinc, Cadmium and Lead doped L-Threonine Manganese Acetate novel single crystals were effectively developed by slow evaporation method. The different portrayals have been done and those properties of both crystals were detailed.

## 2. Materials and Methods

### *2.1. Synthesis*

AR grade chemicals of L-Threonine and Manganese (II) acetate tetra hydrate in the ratio of 1:1 Molar ratio taken in 10ml distilled water and In continues, 0.2M of (AR grade) Zinc (II) acetate (ZnA), Cadmium (II) acetate (CdA) and Lead (II) acetate (PbA) added in 1:0.8 M ratio of L-Threonine and Manganese (II) Acetate solution taken in 10ml distilled water separately each with maintaining the molar ratio as 1:1. All the prepared saturated solutions was filtered and then housed in a dust free atmosphere. The pure LTMA Single crystal and $Zn^{2+}$ doped LTMA, $Cd^{2+}$ doped LTMA and $Pb^{2+}$ doped LTMA single crystals were successfully grown at $30^0$C using with slow evaporation technique.

After a period of 25 days, harvested single crystals of 10×3×2 $mm^3$ size pure LTMA single crystal, 10×4×2 $mm^3$ size of $Zn^{2+}$ doped LTMA, 10×3×2 $mm^3$ size of $Cd^{2+}$ doped LTMA and 10×3×2 $mm^3$ size of $Pb^{2+}$ doped LTMA were grown as shown in Figure 1.

The chemical formula for this process is given below:

Pure LTMA single crystal

$$C_4H_9NO_3+(CH_3COO)_2Mn.4H_2O$$

$$\rightarrow Mn[C_4H_9NO_3]^+2(CH_3COO)^-+4H_2O\uparrow \quad (1)$$

0.2M $(X)^{2+}$ doped LTMA single crystal

$$C_4H_9NO_3+8M(CH_3COO)_{2.}Mn.4H_2O+0.2M(CH_3COO)_2(X) \rightarrow (Mn_{0.8}[C_4H_9NO_3](X)_{0.2})^+ \cdot 2(CH_3COO)^-+ 4H_2O\uparrow \quad (2)$$

(Where X is substituted by $Zn^{2+}$/ $Cd^{2+}$/ $Pb^{2+}$)


Fig 1 As grown (a) Pure LTMA (b) $Zn^{2+}$ doped LTMA (c) $Cd^{2+}$ doped LTMA (d) $Pb^{2+}$ doped LTMA single crystals

## 3. Results and Discussion

This chapter deals with the characterization techniques of the single crystal. These techniques help to study the qualitative nature of the grown single crystal. It will also study the details or presence of chemicals and its activities and performance inside the material. This chapter will help to study the entire ability of the grown material. In general the characterization only exposes the exact nature and effective ability of the material. Based on the technical studies only to the material glittered in the using fields, such as mechanical, electrical and others. In fact, the grown crystal was succeeding by the way of full-fledged studies. Behaviors of a crystal very importantly with its qualitative chemical ratios, dimension, imperfections and the study of its electronic application, stable hardness **(**non-electrical**)**, thermo gravimetric and lighting properties studies. Therefore, to find characterization, this grown pure LTMA and doped LTMA single crystal subjected to studied Single XRD study, Powder XRD study, Energy Dispersive X-ray Analysis (EDAX), Fourier transform infrared (FT-IR), UV-Visible absorbance spectral analysis, and etc.

In the present investigation, the grown crystals were subjected to crystallographic analysis like X-ray diffraction (XRD) study to determine the crystal system and its lattice parameters. The Energy Dispersive X-ray Analysis (EDAX) shows the presence of constituent elements. The functional groups and vibrational frequencies were identified using Fourier transform infrared (FT-IR) spectral analyses. The UV-Visible absorbance spectra were recorded to find out the cut-off wavelength and band gap between the compositions. The Photoluminescence and second harmonic generation nature of the crystal for NLO application are determined and Microhardness test was performed to evaluate the mechanical strength of the material.

### *3.1. Single crystal X-ray diffraction analysis*

Single crystal X-ray diffraction study has been completed for find the crystallinity and for determining the unit cell datas of the grown crystals. It proven as result that the all pure and doped single crystals become same orthorhombic crystal type and which categorized to non-centro-symmetric. The unit cell parameters for pure LTMA and $Zn^{2+}$doped LTMA, $Cd^{2+}$ doped LTMA and $Pb^{2+}$ doped LTMA single crystals are given in Table 1. The volume of the pure LTMA become 530(4) $Å^3$ and all the doped crystals were increased as 538 $Å^3$ for $Zn^{2+}$doped LTMA, 540 $Å^3$ for $Cd^{2+}$ doped LTMA and 540.8(4) $Å^3$ for $Pb^{2+}$ doped LTMA.

Table 1; Lattice parameters of Pure LTMA and $Zn^{2+}$, $Cd^{2+}$ and $Pb^{2+}$ doped LTMA Single crystals

| Lattice parameters | Pure LTMA | $Zn^{2+}$ doped LTMA | $Cd^{2+}$ doped LTMA | $Pb^{2+}$ doped LTMA |
|---|---|---|---|---|
| a | 5.106(19) Å | 5.17 Å | 5.14 Å | 5.147(3) Å |
| b | 7.721(19) Å | 7.71 Å | 7.72 Å | 7.731(2) Å |
| b | 13.45(4) Å | 13.59 Å | 13.60 Å | 13.590(10) Å |
| α=β=γ | 90° | 90° | 90° | 90° |
| Volume | 530(4) $Å^3$ | 538 $Å^3$ | 540 $Å^3$ | 540.8(4) $Å^3$ |
| System | Orthorhombic | Orthorhombic | Orthorhombic | Orthorhombic |
| Space group | $P_{212121}$ | $P_{212121}$ | $P_{212121}$ | $P_{212121}$ |

### *3.2. Powder XRD analysis*

The Powder XRD pattern of pure LTMA and $Zn^{2+}$, $Cd^{2+}$ and $Pb^{2+}$ doped LTMA Single crystals were plotted as shown in Fig. 2. All the doped Powder XRD patterns are clearly differs with different peaks reaction of dopants, the similarities and differences between the pure and doping crystals are well known in variations of patterns in Figure. 2. The inner reagent of Zinc (II) acetate (ZnA), Cadmium (II) acetate (CdA) and Lead (II) acetate (PbA) were well mixing with the Manganese (II) acetate (MnA) as 0.2 M and 0.8 M ratio. This perfect mixture results that without changing the pure LTMA crystal structure Orthorhombic crystal system and all the $Zn^{2+}$ doped LTMA, $Cd^{2+}$ doped LTMA and $Pb^{2+}$ doped LTMA Single crystals also become as same Orthorhombic crystal system. The hkl planes of Pure LTMA and $Zn^{2+}$, $Cd^{2+}$ and $Pb^{2+}$ doped LTMA single crystals with respective 2θ values are calculated tabulated in Table 3, 4 & Table 5.

Therefore, 0.2M dopant of $Zn^{2+}$, $Cd^{2+}$ and $Pb^{2+}$ doped LTMA Single crystals, the first peak remains the same maximum peak level from pure LTMA is 1163 a.m.u and 1184 a.m.u, 1029 a.m.u & 1184 a.m.u for $Zn^{2+}$ doped LTMA, $Cd^{2+}$ doped LTMA and $Pb^{2+}$ doped LTMA Single crystals respectively. Most of the peaks are differed with different 2θ values. Several peaks are repeated in different 2θ values.

### *3.3. EDAX analysis*

Energy dispersive spectroscopy is a chemical microanalysis technique working in combination with Quanta 200 FEG scanning electron microscope (Figure 2.3). The interaction of the electron beam with a specimen in the scanning electron microscope produces many results, including X-rays. Some of the X-rays produced in this manner have wavelength and energies those are determine characteristics of the element of that specimen. It is a technique used to found the elemental composition of the sample. Elemental evaluation by the analytical microscopy may be accomplished with the help of analyzing the emitted radiation and result that those specific wavelengths are absorbed. All the crystals were subjected to energy dispersive analysis. Elements are determined and displayed as atomic percentile. Energy achievements correspond to the related elements with positioning in pure and doped LTMA crystals is shown in the Fig. 3(a) and (b), (c), (d). In the EDAX analysis, it was observed that the presence of $Mn^{2+}$ in pure LTMA single crystal and $Mn^{2+}$. In doped LTMA single crystals all the dopant $Zn^{2+}$, $Cd^{2+}$ and $Pb^{2+}$ are presents. The values of EDAX Spectra reported in Table.6, 7, 8 and 9.

Table.2; hkl planes of Pure LTMA single crystal

| 20 | Intensity | hkl |
|---|---|---|
| 4.0 | 1163 | 111 |
| 8.8 | 93 | 211 |
| 12.5 | 134 | 222 |
| 17.6 | 100 | 411 |
| 22.2 | 345 | 422 |
| 25.6 | 154 | 431 |
| 26.6 | 203 | 444 |
| 36.0 | 108 | 552 |
| 38.4 | 113 | 661 |

Table.3 hkl planes of $Zn^{2+}$ doped Pure LTMA single crystal

| 2θ | Intensity | Hkl |
|---|---|---|
| 4.1 | 1184 | 111 |
| 12.6 | 100 | 211 |
| 17.6 | 160 | 220 |
| 19.6 | 173 | 221 |
| 20.6 | 384 | 301 |
| 21.0 | 199 | 311 |
| 22.6 | 147 | 222 |
| 25.6 | 151 | 302 |
| 28.0 | 108 | 321 |
| 29.0 | 182 | 322 |
| 31.0 | 139 | 402 |
| 34.0 | 104 | 422 |
| 36.0 | 95.9 | 432 |
| 38.8 | 78.8 | 521 |
| 41.8 | 104.5 | 532 |

Table.4 hkl planes of $Cd^{2+}$ doped Pure LTMA single crystal

| 2θ | Intensity | hkl |
|---|---|---|
| 4.1 | 1029 | 111 |
| 13.1 | 230 | 211 |
| 18.2 | 157.4 | 311 |
| 20.2 | 256.7 | 222 |
| 20.6 | 235.0 | 321 |
| 21.5 | 187.8 | 322 |
| 22.2 | 174.8 | 331 |
| 22.9 | 230.7 | 421 |
| 23.5 | 144.9 | 422 |
| 23.9 | 200.8 | 500 |
| 28.6 | 252.4 | 521 |
| 29.2 | 157.0 | 440 |
| 35.0 | 93.3 | 442 |
| 37.3 | 127.6 | 543 |
| 39.0 | 100 | 551 |

### *3.4. Fourier Transform Infra-Red analysis*

The FTIR spectrum of Pure and doped LTMA crystals were obtained as shown in Fig. 4. The placing of $NH^{3+}$ is clearly identified in the FT-IR spectrum by the wide intense with the respective data as 3169.25$cm^{-1}$ relating to asymmetric vibration mode of $NH_3^+$. The opposite symmetric vibration band lies as frequency of 3029.80 $cm^{-1}$. The both symmetric and asymmetric bending vibrations appear as 1417.94 $cm^{-1}$ and 1629.28 $cm^{-1}$. CH symmetric deformation appears in 1346.04$cm^{-1}$ respectively.$NH_3^+$ Rocking, C-N Rocking, C-C Rocking and C-C-N Rocking appear in 1113.14$cm^{-1}$.1040.72$cm^{-1}$, 932.53$cm^{-1}$ and 871.20$cm^{-1}$. 769.77 $cm^{-1}$ indicates $COO^-$ Bending, 701.35 $cm^{-1}$ and 560.11$cm^{-1}$ indicates the $COO^-$ wagging vibration and $COO^-$ Rocking Deformation respectively. $NH_3^+$ Bending appears at 489.82 $cm^{-1}$.The OCO rocking frequency found out at 445.18 $cm^{-1}$.

Table.5 hkl planes of $Pb^{2+}$ doped Pure LTMA single crystal

| 2θ | Intensity | hkl |
|---|---|---|
| 3.93 | 1178 | 111 |
| 12.5 | 134 | 211 |
| 17.6 | 100 | 222 |
| 22.2 | 345 | 411 |
| 25.6 | 154 | 422 |
| 26.6 | 203 | 431 |
| 36.0 | 108 | 444 |
| 38.4 | 113 | 552 |
| 44.9 | 176 | 661 |

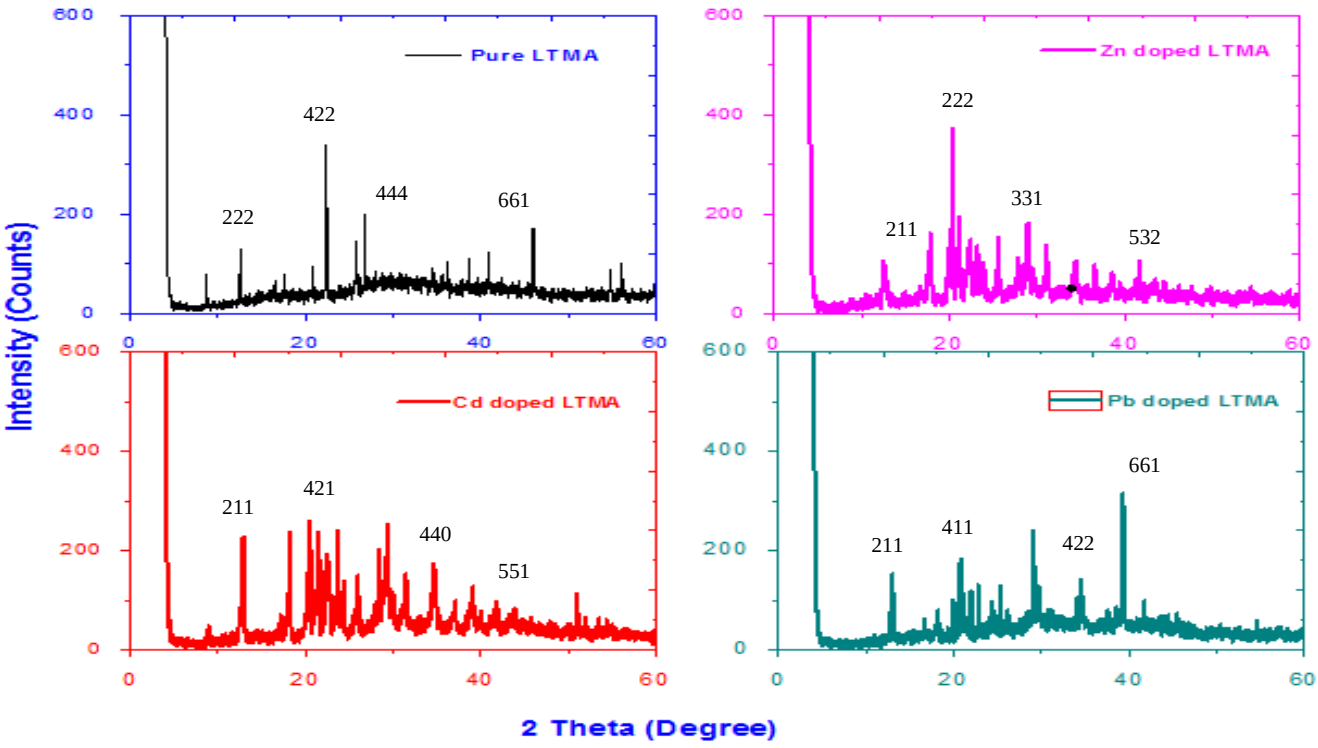


Fig. 2 XRD plotting of pure LTMA and $Zn^{2+}$, $Cd^{2+}$ and $Pb^{2+}$ doped LTMA

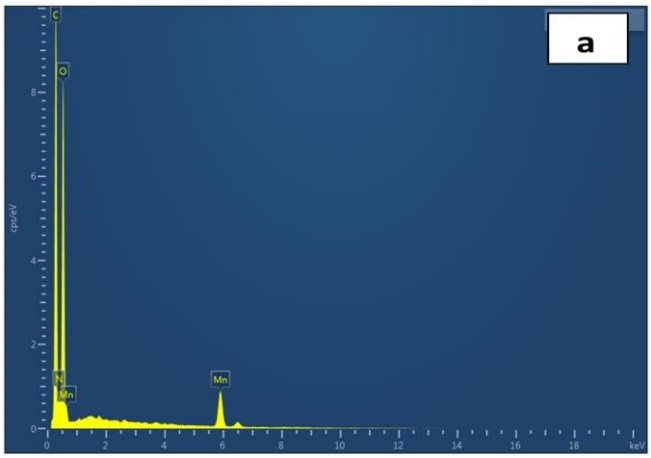


Fig. 3 Energy dispersive Spectra of (a) Pure LTMA

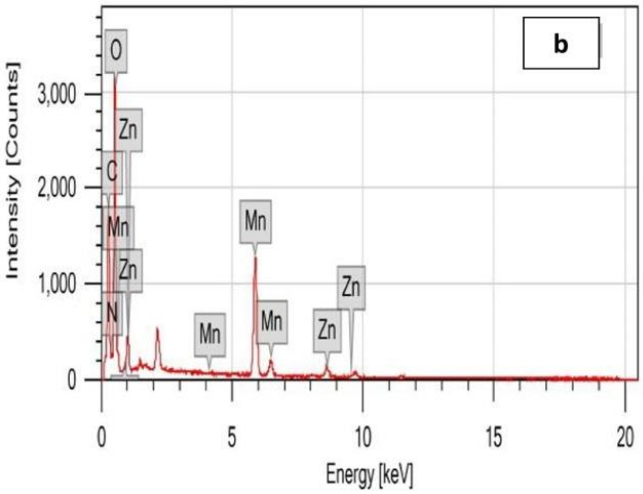


Fig. 4 Energy dispersive Spectra of (b) $Zn^{2+}$ doped LTMA

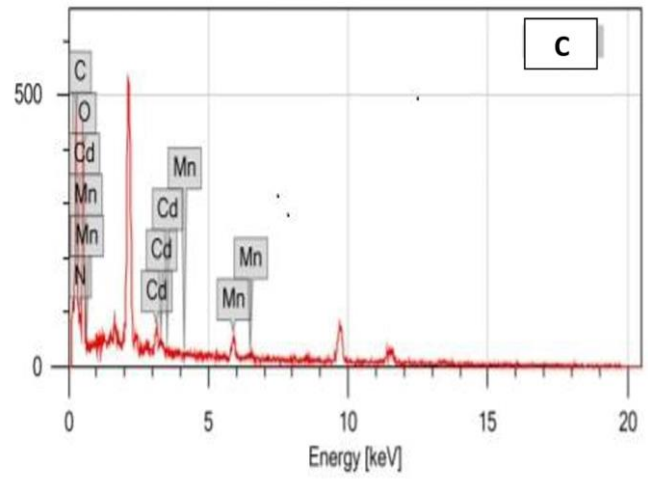


Fig. 5 Energy dispersive Spectra of (c) $Cd^{2+}$ doped LTMA

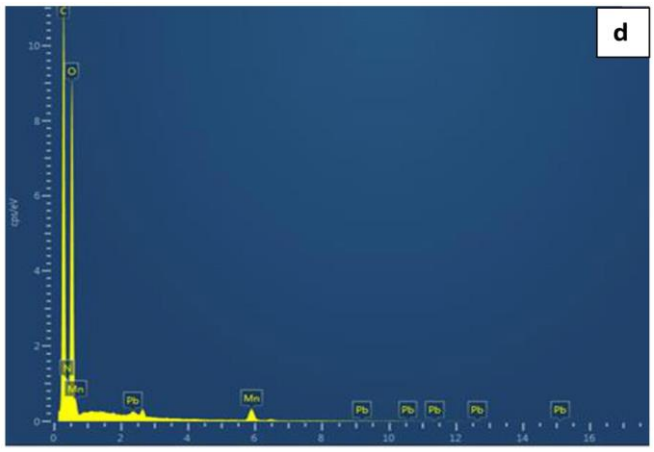


Fig. 6 Energy dispersive Spectra of (d) $Pb^{2+}$ doped LTMA Single Crystal

Table.6 EDAX report of Pure LTMA

| Element | Line Type | Wt% | Atomic % |
|---|---|---|---|
| Carbon | K | 41.51 | 49.7 |
| Nitrogen | K | 6.76 | 6.94 |
| Oxygen | K | 46.79 | 42.06 |
| Manganese | K | 4.94 | 1.29 |
| Total: | | 100 | 100 |

Table.7 EDAX report of (b) $Zn^{2+}$ doped LTMA

| Element | Line Type | Wt% | Atomic % |
|---|---|---|---|
| Carbon | K | 36.47±0.19 | 51.73±0.26 |
| Nitrogen | K | 0.34±0.14 | 0.41±0.17 |
| Oxygen | K | 37.73±0.28 4 | 40.17±0.30 |
| Manganese | K | 21.24±0.22 | 6.59±0.07 |
| Zinc | K | 4.22±0.16 | 1.10±0.04 |
| Total: | | 100 | 100 |

Table.8 EDAX report of $Cd^{2+}$ doped LTMA

| Element | Line Type | Wt% | Atomic % |
|---|---|---|---|
| Carbon | K | 38.65 | 48.04 |
| Nitrogen | K | 7.75 | 8.26 |
| Oxygen | K | 45.04 | 42.03 |
| Manganese | K | 3.85 | 1.05 |
| Cadmium | L | 4.70 | 0.62 |
| Total: | | 100 | 100 |

Table.9 EDAX report of $Pb^{2+}$ doped LTMA

| Element | Line Type | Wt% | Atomic % |
|---|---|---|---|
| Carbon | K | 40.33 | 47.47 |
| Nitrogen | K | 9.14 | 9.22 |
| Oxygen | K | 48.55 | 42.9 |
| Manganese | K | 1.45 | 0.37 |
| Lead | M | 0.54 | 0.04 |
| Total: | | 100 | 100 |

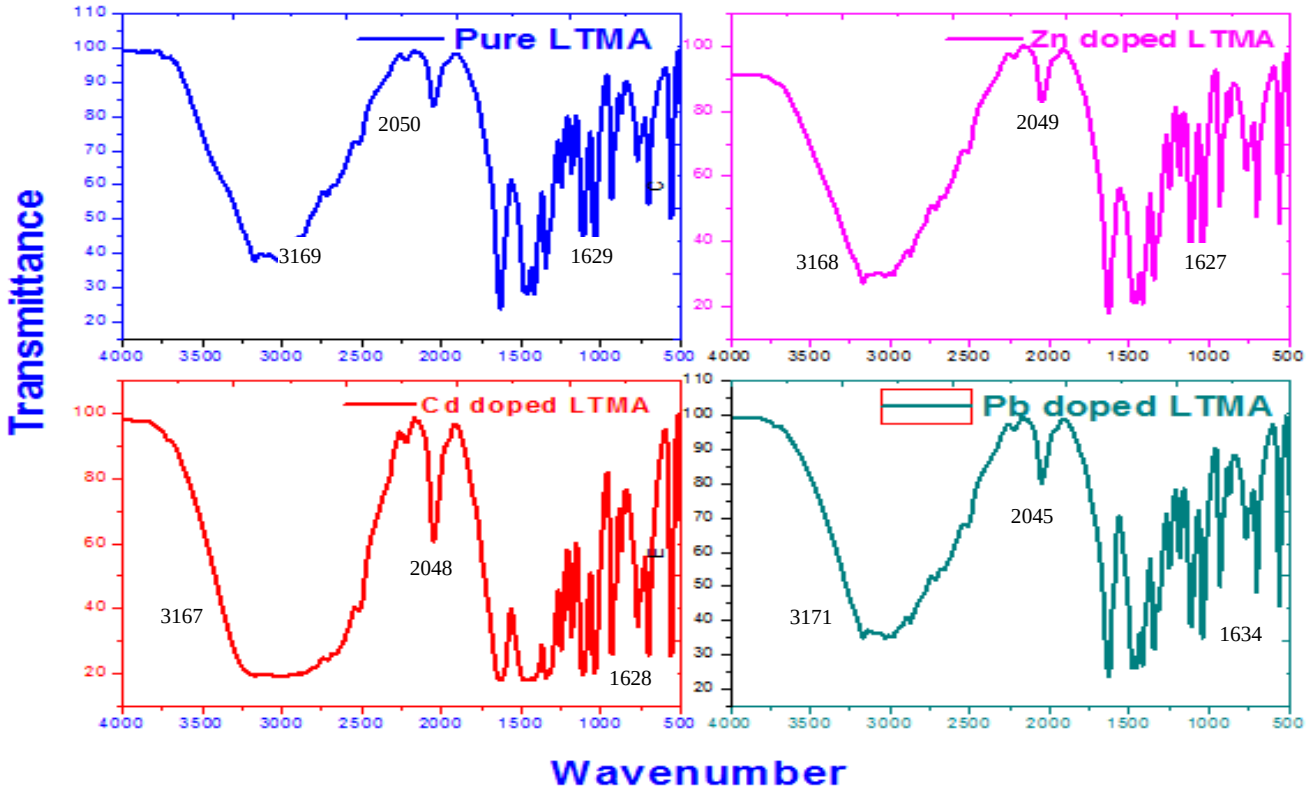


Fig. 7 FTIR Spectrum of Pure LTMA and $Zn^{2+}$, $Cd^{2+}$ and $Pb^{2+}$ doped LTMA

### *3.5. Optical Studies:*

#### *3.5.1. UV- Absorption & Transmittance analysis*

UV-Visible spectrum is the tracing of the penetration of the light beam when it passes through a powder or when getting reflection on sample surface. The optical transmission spectra are recorded for polished plates of grown crystals using VARIAN CARY 5E UV-Vis-NIR Spectrophotometer. The spectrophotometer makes the monochromatic beam which resolves radiation into its relating wavelengths, samples occupation and also detector which ensures the amount of beam transited on the sample. Two light sources are used to cover entire range of spectrum from 200-2500 nm. A straightened bandwidth was selected using with band pass filters. Then the radiation was repeatedly passed with the cells of the given phenomenon alternatively and respectively. This double beam process eliminates that the fluctuations on intensity of scattering radiation and solvent effects. The two rays were combined and differences in intensities of those two radiations are measured electrically. The displacement of the monochromator and the recorder were compiled and adjusted to that the recording the maximum effectual light of appropriate radiation. The transmission study aimed to recording the insensible beam in terms of percentage of transmittance along with Y-axis and related the wavelength (nm) along X-axis. The UV-Visible spectrum implies that the information as the useful range of wavelength in which the NLO materials has been obtain. The recorded UV-transmittance plots of Pure and doped LTMA crystals were shown in Fig. 5. Observed transmittance spectrum is well cutoff for both pure and doped crystals which conclude as ignoring of NLO property material. UV absorption plot shows that the lower cut off λ 267 nm and around 200 nm for Pure and doped crystals respectively. The lower cut-off λ resulted that the very clear transparency, implies the use of material as electro optical devices, because the lower cutoff wavelength is 200nm and this character easily causes the NLO nature [25]. The energy band gap is calculated using the formula for pure crystal as 4.6eVand for the $Zn^{2+}$, $Cd^{2+}$ and $Pb^{2+}$ doped crystal as 6.3eV, 6.45eV and 6.5eV as shown in fig 6.

$$E_g=1240/\lambda \quad (3)$$

Table 10 FTIR Spectral Assignment of Pure LTMA and $Zn^{2+}$, $Cd^{2+}$ and $Pb^{2+}$ doped LTMA Single Crystals

| Wavenumber Pure L-Threonine [Reported 14] | Pure LTMA | $Zn^{2+}$ doped LTMA | $Cd^{2+}$ doped LTMA | $Pb^{2+}$ doped LTMA | Assignment |
|---|---|---|---|---|---|
| - | 3169.25 | 3168.09 | 3167.43 | 3171 | $NH_3^+$ asymmetric stretching |
| - | 3029.80 | 3028.32 | 3027.75 | 3028.16 | $NH_3^+$ symmetric stretching |
| 1625.99 | 1629.28 | 1627.65 | 1628.20 | 1634 | $NH_3^+$ asymmetric deformation |
| 1417 | 1417.94 | 1417.16 | 1417.01 | 1413 | $NH_3^+$ symmetric deformation |
| 1346.48 | 1346.04 | 1345.48 | 1345.17 | 1343 | CH symmetric deformation |
| -- | 1113.14 | 1112.73 | 1112.90 | 1112 | $NH_3^+$ Rocking |
| 1040.52 | 1040.72 | 1040.89 | 1040.62 | 1051 | C-N Rocking |
| 931.50 | 932.53 | 932.33 | 932.31 | 921 | C-C Rocking |
| 871.09 | 871.20 | 870.76 | 870.92 | 871.29 | C-C-N Rocking |
| 767.90 | 769.77 | 769.12 | 769.20 | 769.05 | $COO^-$ Bending |
| 701.52 | 701.35 | 701.10 | 701.16 | 700 | $COO^-$ wagging vibration |
| 560.19 C | 560.11 | 559.90 | 559.85 | 549 | $COO^-$ Rocking Deformation |
| 489.64 | 489.82 | 489.30 | 489.75 | 490.02 | $NH_3^+$ Bending |
| - | 445..18 | 444.79 | 445.36 | 445.89 | In plan OCO Rocking |

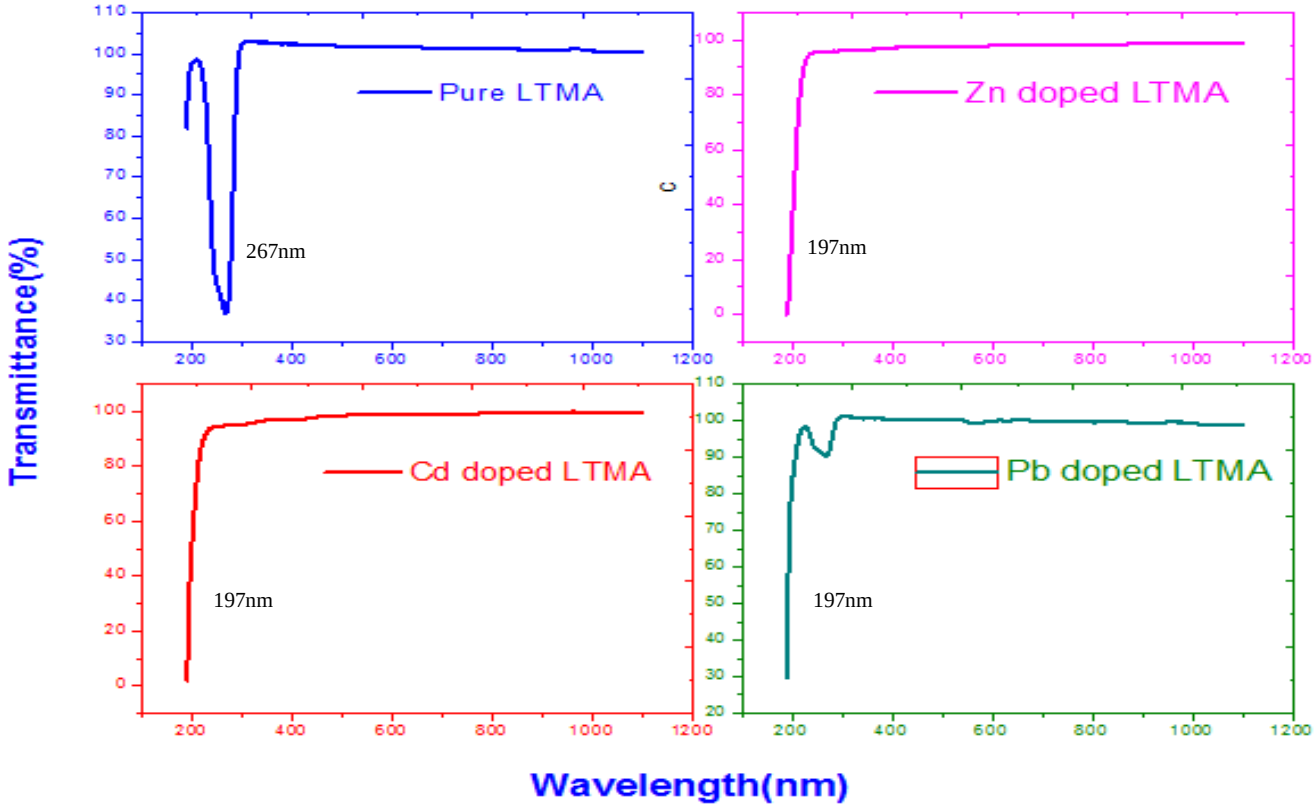


Fig. 8 The UV-Visible Transmittance Spectra of Pure and $Zn^{2+}$, $Cd^{2+}$ and $Pb^{2+}$ doped LTMA

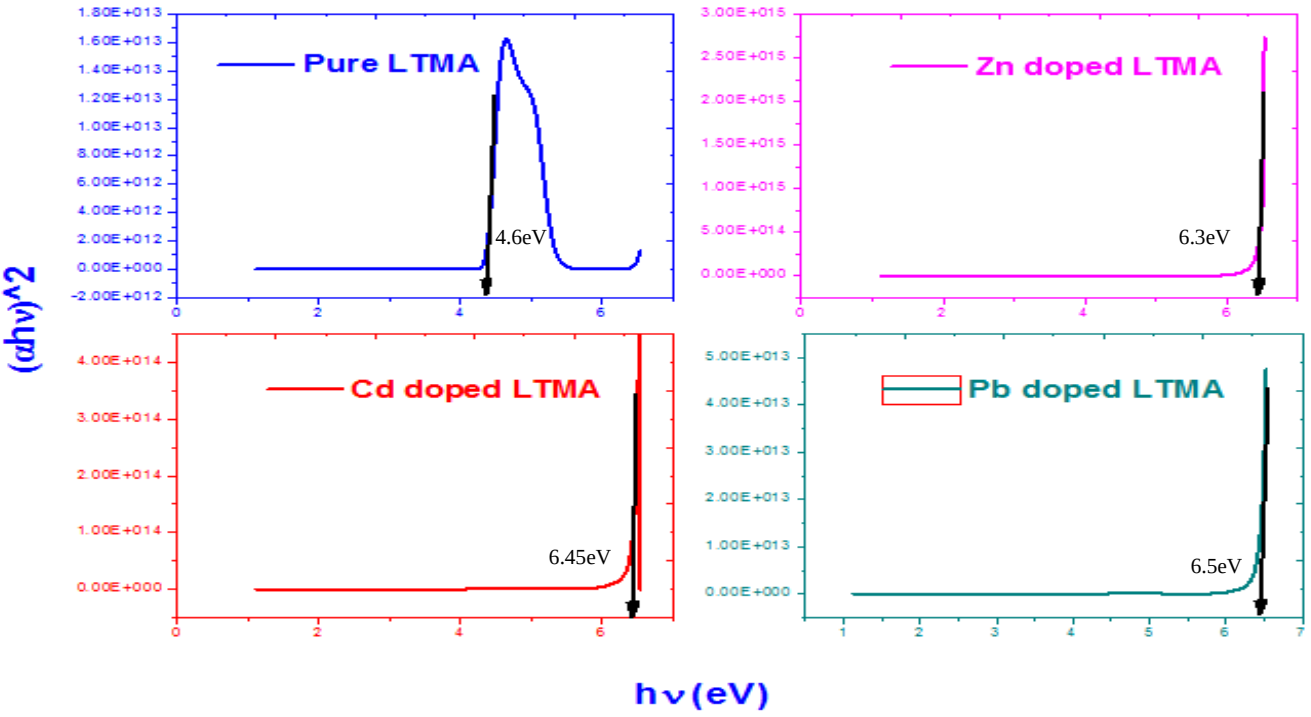


Fig. 9 Energy band gap Spectra of Pure and $Zn^{2+}$, $Cd^{2+}$ and $Pb^{2+}$ doped LTMA

*3.6 Vicker's Microhardness Analysis*

Microhardness study was obtained for determining the roughness of the all the grown crystals with HMT 2T, SHIMADZU. The indentation mark is determined on the all crystals at $30^0$C by applying load 25gm, 50gm and 100 gm. The hardness value $H_v$ was determined as increases with the increase in mechanical stress applied from 25gm to 100 gm and crack resulted at higher loads. Vicker's microhardness number $H_v$ of the crystals was calculated using the following equation

$$H_v = 1.8544\ P/d^2\ (kg/mm^2) \qquad (4)$$

Where, $H_v$ - Vicker's hardness number in $kg/mm^2$, P – mechanical stress and d - average diagonal distance of the indentation. From the graph, observed that the hardness value of all the doping crystals increased with small bends up to 100 gm. So, all the hardness numbers of $Zn^{2+}$, $Cd^{2+}$ and $Pb^{2+}$ doped LTMA material increased and the datas are reported in Table 11.

Table 11 Hardness values of Pure LTMA and doped LTMA Single Crystals

| Load (gm) | P | Hardness ($H_V$) | | | |
|---|---|---|---|---|---|
| | | Pure LTMA | $Zn^{2+}$ doped LTMA | $Cd^{2+}$ doped LTMA | $Pb^{2+}$ doped LTMA |
| 25 | | 37 | 29.34 | 27.6 | 29.85 |
| 50 | | 50.8 | 40.8 | 30.2 | 49.65 |
| 100 | | 80.5 | 57.7 | 43.35 | 78.6 |

*3.7. Photoluminescence Study (PL)*

The grown pure LTMA and 0.2M of $Zn^{2+}$ doped LTMA, $Cd^{2+}$ doped LTMA, $Pb^{2+}$ doped LTMA crystals resulted that under situated to PL Study, it (Fig.10) reveals that the Emission spectrum at 486.96nm as respectively.

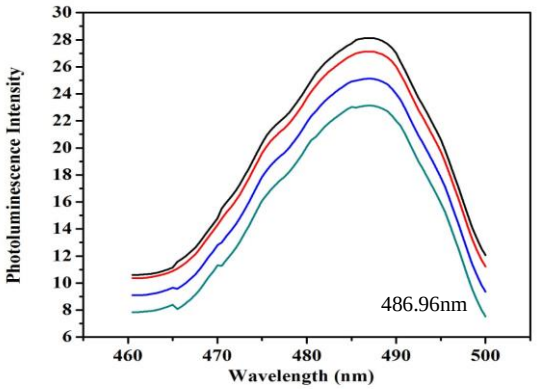


Fig. 10 PL spectrum of Pure and doped LTMA crystal.

## 4. Conclusions

Novel Single crystals of undoped and inner doped L-Threonine Manganese Acetate were effectively developed with spontaneous evaporation. Single precious crystal study examines structure of the all the crystals becomes

Orthorhombic and has bigger volume from $530^0A^3$ to $540.8^0A^3$. The powder diffraction examinations were done the crystallinity contrasts between the unadulterated and inner doped LTMA single crystal. EDAX study affirmed the presence of the dopant Mn in Pure LTMA and Zn, Cd and Pb in doped Crystal. UV-study found the unadulterated and all the doped crystals have wide straightforwardness in entire noticeable area and utilizing with their vitality band holes 4.6eV and 6.3eV, 6.45eV and 6.5V were resolved. FTIR considers uncover that the nearness of utilitarian gatherings in the crystals. The enormous changes in mechanical quality of the pure and doped crystals were concentrated by Vicker's Micro hardness analyzer. PL emission spectrum wave length 486.96nm of Pure and doped LTMA crystal also determined

**Acknowledgment**

I express my sincere Thanks to SAIF, IIT-Madras, Tamil Nadu, India, SAIF, Cochin-Kerala, India and St. Joseph's College, Tiruchirappalli, Tamil Nadu, India, for kind co-operation of sending the test results on time, helps to completing the research work.

**References**

[1] ML Caroline, S Vasudevan, "Growth and characterization of an organic nonlinear optical material" L-alanine alaninium nitrate, Materials Letters, vol. 62, p.p. 2245–2248, (2008).

[2] S. Dhanuskodi, J. Ramajothi, "Crystal Growth, thermal and optical studies of L-Histidine Tetrafluoroborate-a Semi Organic NLO materials", Cryst. Res. Technol., vol. (39) 7, p.p. 592 – 597, (2004)

[3] D. Eimerl, S. Velsko, L. Davis, F. Wang, J. Loiacono, F. Kennedy, "Deuterated L-Arginine phosphate: a new efficient nonlinear crystal", IEEE J. Quantum Electron, vol. (25) 2 , p.p. 179 – 193, (1989).

[4] D Geetha, M Prakash, ML Caroline, PS Ramesh, "Growth and characterization of the nonlinear optical single crystal" L-Phenylalanine-benzoic acid, Adv. Appl. Sci. Res., vol. (2) 2, p.p. 86-92, (2011).

[5] V Ananthanarayanan, "Raman Spectra Of Single Crystals Of Zinc And Lithium Acetate Dihydrate", vol. (56) 4, p.p. 188-197, (1962).

[6] Arii, Tadashi, Kishi, Akira, "The effect of humidity on thermal process of zinc acetate", Thermochimica Acta, vol. 400 (1-2), p.p. 175-185, (2003).

[7] K. Arun and S. Jayalekshmi, "Growth and Characterization of Nonlinear Optical Single Crystals of L-Alaninium Oxalate," Journal of Minerals and Materials Characterization and Engineering, vol. (8)8, p.p. 635-646, (2009).

[8] [8] Balakrishnan. T and Ramamurthi.K, "Growth and characterization of glycine lithium sulphate single Crystal", Crystal Research and Technology, vol. 41(12),p.p. 1184 – 1188, (2006).

[9] D. Balasubramanian, P. Murugakoothan, R. Jayavel, "Synthesis, growth and characterization of organic nonlinear optical bis-glycine maleate (BGM) single crystals", Journal of Crystal Growth, vol. (312) 11, p.p. 1855-1859, (2010).

[10] J.H. Joshi, S. Kalainathan, D.K. Kanchan, M.J. Joshi, K.D. Parikh, "Effect of L-Threonine on growth and properties of ammonium dihydrogen phosphate crystal", Arabian Journal of Chemistry, vol. (13), p.p. 1533-1550, (2020).

[11] Dhas, Martin Britto. S. A, Suresh. M, Raji. P, Ramachandran. K and Natarajan. S, "Photoacoustic studies on two new organic NLO materials:L-threonine and L-prolinium tartrate", Crystal Research and Technology, vol. 42(2), p.p. 190-194, (2007).

[12] Gunasekaran. S and Ramkumar. G. R, "Analysis on Suitability of Pure and α-Histidine Doped KDP Crystals in High Speed Applications", Indian Journal of Physics, vol. 83, p.p. 1549, (2009).

[13] Hwang, Cheong-Soo, Lee, Narae, Kim, Young-Ah, Park, Youn Bong, "Synthesis of the Water Dispersible L-Valine Capped ZnS:Mn Nano crystal and the Crystal Structure of the Precursor Complex: $Zn(Val)2(H2O)^+$ ", Bull. Korean Chem. Soc., vol (27)11, p.p. 1809-1814, (2006).

[14] G. Ramesh Kumar, S. Gokul Raja, R. Mohana, R. Jayavel, "Growth, structural and spectral analyses of nonlinear optical L-Threonine single crystals", Journal of Crystal Growth, vol. 275, p.p. 1947–1951, (2005).

[15] N. Indumathi, K. Deepa, S. Senthil, "Growth and characterization of L-Threonine Lithium Chloride:A New semi organic Non Linear Optical single crystal", IJEDR, vol. (8)1, p.p. 560-564, (2017).

[16] R. Vivekanandhan, K. Raju, S. Sahaya Jude Dhas, V. Chidambaram, "Investigation of Novel Nonlinear Optical L-Threonine Calcium Chloride Single Crystal Grown by Solution Growth Technique", International Journal of Applied Engineering Research, vol. (13)18, p.p. 13454-13459, (2018).

[17] S. Masilamani, A. Mohamed Musthafa, P. Krishnamurthi, "Synthesis, growth and characterization of a semiorganic nonlinear optical material: L-Threonine Cadmium Chloride single crystals", vol. (10)2, p.p. S3962-S3966, (2017).

[18] C. Vijayaraj, M. Mariappan, G. Nedunchezhian, D. Benny Anburaj and B. Gokulakumar, "Synthesis Growth and Characterization of a New NLO Material: L-Threonine Manganese Chloride" Indo – Asian Journal of Multidisciplinary Research (IAJMR), vol. (2)2, p.p. 555-560, (2018).

[19] J. Elberin Mary Theras, D. Kalaivani, J. Arul Martin Mani, D. Jayaraman, V. Joseph, "Synthesis, structural and optical properties, ferromagnetic behaviour,

cytotoxicity and NLO activity of lithium sulphate doped L-Threonine", Optics & Laser Technology, vol. 83, p.p. 49-54, (2016).

[20] T. Manimaran, P. Paramasivam, S. Bhuvaneswari, R.S. Abina Shiny, B. Ravindran & M. Mariappan, "Growth and Characterization of L-Threonine Potassium Sulphate" A New NLO Semi Organic Crystal, Research Review Journal, vol. (04)03, p.p. 644-647, (2019).

[21] S.A.D. Christopher, N.N.K. Pillai, "Growth and Structural studies of Zn doped L-Threonine single crystal", IJES, vol. (4)8, p.p. 01-04, (2015).

[22] M. Nagarajan, N. Neela kanda Pillai, S. Perumal, "Growth and Structural studies of Cu doped L-Threonine single crystal", IJLTEMAS, vol. (IV)XI, p.p. 7-11, (2015).

[23] M. Abila Jeba Queen, K. C. Bright, S. Mary Delphine, P. Aji Udhaya, "Spectroscopic Investigation of supramolecular-organometallic compound L-Threonine Cadmium Acetate Monohydrate", Spectrochemica Acta Part A: Molecular and Biomolecular Spectroscopy, vol. (19), p.p. S1386-1425, (2019).

[24] A. Puhal Raj, C. Ramachandra Raja, "Synthesis, Growth, Structural, Spectroscopic, Thermal and Optical Properties of NLO Single Crystal L-Threonine Zinc Acetate", Photonics and Optoelectronics (P&O), vol. 3, p.p. 56-64, (2013).

[25] K. Sudhakar, S. Muniyappan, P. Murugakoothan, "Growth and Characterization of a Potential Organic NLO Single Crystal: Guanidinium 4-AminobenzeneSulfonate (GuAS) ", materials today: Proceedings, (8)1, p.p. 256-263, (2019).